Alcohol-induced defects in hepatic transcytosis may be explained by impaired dynein function

Jennifer L. Groebner,
Department of Biology, The Catholic University of America, 620 Michigan Avenue, NE, Washington, DC 20064, USA

David J. Fernandez,
Department of Biology, The Catholic University of America, 620 Michigan Avenue, NE, Washington, DC 20064, USA

Dean J. Tuma, and
Department of Internal Medicine, University of Nebraska, Omaha, NE 68105, USA

Pamela L. Tuma
Department of Biology, The Catholic University of America, 620 Michigan Avenue, NE, Washington, DC 20064, USA

Abstract

Alcoholic liver disease has been clinically well described, but the molecular mechanisms leading to hepatotoxicity have not been fully elucidated. Previously, we determined that microtubules are hyperacetylated and more stable in ethanol-treated WIF-B cells, VL-17A cells, liver slices, and in livers from ethanol-fed rats. From our recent studies, we believe that these modifications can explain alcohol-induced defects in microtubule motor-dependent protein trafficking including nuclear translocation of a subset of transcription factors. Since cytoplasmic dynein/dynactin is known to mediate both microtubule-dependent translocation and basolateral to apical/canalicular transcytosis, we predicted that transcytosis is impaired in ethanol-treated hepatic cells. We monitored transcytosis of three classes of newly synthesized canalicular proteins in polarized, hepatic WIF-B cells, an emerging model system for the study of liver disease. As predicted, canalicular delivery of all proteins tested was impaired in ethanol-treated cells. Unlike in control cells, transcytosing proteins were observed in discrete sub-canalicular puncta en route to the canalicular surface that aligned along acetylated microtubules. We further determined that the stalled transcytosing proteins colocalized with dynein/dynactin in treated cells. No changes in vesicle association were observed for either dynein or dynactin in ethanol-treated cells, but significantly enhanced dynein binding to micro-tubules was observed. From these results, we

tuma@cua.edu.
Present Address: D. J. Fernandez, Northern Virginia Community College, Annandale, VA 22003-3796, USA

propose that enhanced dynein binding to microtubules in ethanol-treated cells leads to decreased motor processivity resulting in vesicle stalling and in impaired canalicular delivery. Our studies also importantly indicate that modulating cellular acetylation levels with clinically tolerated deacetylase agonists may be a novel therapeutic strategy for treating alcoholic liver disease.

Keywords

Dynactin; Dynein; Ethanol; Microtubules; Transcytosis; WIF-B cells

Introduction

The liver is the primary site of ethanol metabolism and thus sustains the most tissue damage from chronic alcohol consumption. Although the clinical manifestations of alcoholic liver disease have been well characterized, the molecular mechanisms responsible for hepatotoxicity remain ill-defined. Our recent studies have been performed in polarized, hepatic WIF-B cells, an emerging model system for the study of alcoholic liver injury [1, 2] (and see Discussion). After 7–10 days in culture, WIF-B cells fully polarize forming compositionally and functionally distinct basolateral/sinusoidal and apical/canalicular membrane surface domains. This allows us to examine polarized protein trafficking in the biosynthetic and endocytic pathways that are lost or absent in other in vitro hepatocyte model systems. Additionally, WIF-B cells highly differentiate in culture exhibiting enumerable adult hepatocyte functions. Importantly for these studies, WIF-B cells efficiently metabolize ethanol with endogenously expressed alcohol dehydrogenase (ADH) and cytochrome P_{450} 2E1 (CYP2E1) [1, 2].

Using this model system, we determined that alcohol exposure leads to increased microtubule acetylation to approximately 3-fold over that of control [3]. This post-translational modification is associated with stable micro-tubules (vs. the more commonly studied dynamic micro-tubules) that are characterized by a longer half-life ($t_{1/2} = 1$ h vs. 10 min) and resistance to microtubule poisons (e.g., cold and nocodazole) [4]. We further determined that increased acetylation correlates with increased microtubule stability and confirmed these findings in VL-17A cells, liver slices, and in livers from ethanol-fed rats indicating that the findings have physiologic importance [3, 5]. Addition of 4-methylpyrazole (an ADH inhibitor) prevented hyperacetylation while addition of cyanamide (an aldehyde dehydrogenase inhibitor) potentiated it [3]. In contrast, diallylsulfide (a CYP2E1 inhibitor) or *N*-acetyl cysteine (an anti-oxidant) addition had no effect on microtubule acetylation (manuscript in preparation). Together these results indicate that only ADH-mediated ethanol metabolism to acetaldehyde contributes to enhanced microtubule acetylation. Because microtubules are central to countless cellular processes ranging from organelle placement to mitosis to vesicle motility, any alterations in their dynamics may have serious ramifications on proper hepatic function. We have been examining the relationship between microtubule dynamics and alcohol-induced defects in protein trafficking.

Work from almost 20 years ago suggested that different microtubule populations (and/or their modifications) support specific protein trafficking steps [6]. Of particular interest, are more recent studies performed in WIF-B cells that used a novel microtubule depolymerizing drug, 201-F [7]. This drug specifically depolymerizes dynamic micro-tubules leaving only stable, acetylated polymers behind. So far, 201-F-treatment has been shown to impair three microtubule-dependent protein trafficking pathways: basolateral to canalicular transcytosis, basolateral secretion from the TGN, and the nuclear translocation of STAT5B [7, 8]. Remarkably, the latter two trafficking pathways are also known to be impaired in ethanol-treated hepatic cells [5, 9]. We have further correlated the ethanol-induced defects in secretion and nuclear translocation to increased microtubule acetylation and stability using two other pharmacological agents: 1) trichostatin A, an agent that leads to global protein acetylation; and 2) taxol, an agent that specifically induces microtubule acetylation [5, 9]. In all cases, the alcohol-induced trafficking defects were impaired to similar extents by the two agents strongly suggesting that alcohol-induced microtubule acetylation is responsible for the defect.

To date, basolateral to canalicular transcytosis has not been examined in ethanol-treated hepatocytes. In an effort to more fully examine the relationship between alcohol-induced microtubule acetylation and impaired protein trafficking, we examined transcytosis of three classes of canalicular proteins in WIF-B cells. Because both STAT5B nuclear translocation and transcytotic vesicle motility are thought to be mediated by cytoplasmic dynein (a minus-end directed microtubule motor) and dynactin (a dynein activating complex) [8], we further examined the distributions and properties of these proteins in control and ethanol-treated cells.

Materials and methods

Reagents

F12 (Coon's) medium, taxol, HRP-conjugated secondary antibodies, and monoclonal antibodies against α-tubulin or acetylated α-tubulin were purchased from Sigma–Aldrich (St. Louis, MO). FBS was from Gemini Bio-Products (Woodland, CA). Hepes and Alexa-488 and -568-conjugated secondary antibodies were purchased from Life Technologies (Carlsbad, CA). Antibodies against dynein intermediate chain and the p150[glued] subunit of dynactin were from Millipore (Temecula, CA) and BD Biosciences (San Jose, CA), respectively. Antibodies against amino-peptidase N (APN), 5′nucleotidase (5′NT), and the myc epitope and recombinant adenoviruses encoding myc-tagged polymeric IgA receptor (pIgA-R) were kindly provided by Dr. Ann Hubbard (Johns Hopkins School of Medicine, Baltimore, MD).

Cell culture, virus production, and infection

WIF-B cells were grown at 37 °C in medium, pH 7.0, supplemented with 5 % FBS, 10 μM hypoxanthine, 40 nM aminopterin, and 1.6 μM thymidine in a humidified 7 % CO_2 incubator [10]. Cells were seeded onto glass cover-slips at 1.3×10^4 cells/cm^2 and grown for 7–10 days until they reached maximum polarity. Cells were treated on day 7 with 50 mM ethanol in medium buffered with 10 mM Hepes, pH 7.0 for 72 h as described [2]. After 48 h

in ethanol, WIF-B cells were infected with recombinant adenoviruses encoding myc-tagged pIgA-R for 1 h at 37 °C as described [11]. The cells were washed with complete medium and incubated an additional 18–20 h in the continued absence or presence of 50 mM ethanol to allow protein expression.

VL-17A cells (provided by Dr. Dahn Clemens, University of Nebraska Medical Center, Omaha, NE) were grown in a 5 % CO_2 incubator at 37 °C in DMEM containing 10 % FBS as described [12]. Cells were infected with pIgA-R recombinant adenovirus for 1 h at 37 °C then incubated in the absence or presence of 50 mM ethanol for 24 h.

Immunofluorescence microscopy

WIF-B cells were fixed on ice with chilled phosphate buffered saline containing 4 % paraformaldehyde for 1 min and permeabilized with ice-cold methanol for 10 min. Cells labeled for dynein or p150 were fixed and permeabilized with methanol at −20 °C for 5 min. Cells were processed for indirect immunofluorescence as described [13]. Cells were visualized by epifluorescence using an Olympus BX60 Fluorescence Microscope (OPELCO, Dulles, VA). Images were taken with a CoolSnap HQ2 digital camera (Photo-metrics, Tucson, AZ) and IPLabs image analysis software (Biovision, Exton, PA). For the colocalization experiments shown in Fig. 5B, cells were visualized using a Zeiss Observer.Z1 Fluorescence Microscope (Zeiss, Thornwood, NY). Images were taken with an AxioCam MRm digital camera using Zen 2012 digital imaging software (Zeiss, Thornwood, NY). Adobe Photoshop (Adobe Systems Inc., Mountain View, CA) was used to compile figures.

Antibody trafficking in live cells

To monitor transcytosis, cells were basolaterally labeled with antibodies specific to APN (1:50), 5′NT (1:100) or myc (1:250; to label pIgA-R) for 20 min at 4 °C. Cells were washed 3 times for 2 min on ice and then reincubated with prewarmed complete medium. Antibody-antigen complexes were chased for 0, 45, or 90 min at 37 °C and processed for immunofluorescence labeling. For the colocalization experiments, APN at the basolateral surface was continuously antibody labeled (1:100) for 45 min at 37 °C. Cells were washed 3 times for 2 min with prewarmed complete medium and processed for epifluorescence imaging. To quantitate the relative distributions of the transcytosing proteins, random fields from each slide were visualized by epifluorescence and digitized as described. From micro-graphs, the average pixel intensity of selected regions of interest placed at the bile canalicular or basolateral surface of the same WIF-B cell were measured using ImageJ Measure ROI tool (National Institutes of Health) [14, 15]. The averaged background pixel intensity was subtracted from each value, and the ratio of bile canalicular to basolateral fluorescence intensity was determined.

To monitor canalicular protein trafficking in VL-17A cells, pIgA-R expressing cells were labeled at 4 °C for 20 min with anti-myc antibodies and washed as described above. Antibody-antigen complexes were chased for 0 or 15 min at 37 °C. To quantitate the relative protein trafficking levels, random fields from each slide were visualized by epifluorescence

and digitized. From micrographs, the number of cells containing intracellular labeling vs. total number of pIgA-R-expressing cells was counted and a percent was calculated.

Western blotting

Laemmli samples were prepared and boiled for 3 min [16]. Proteins were electrophoretically separated using SDS-PAGE, transferred to nitrocellulose, and immunoblotted with antibodies specific to α-tubulin (1:7,500), acetylated-α-tubulin (1:2,000), dynein (1:1,000), or p150 (1:10,000). Immunoreactivity was detected using enhanced chemiluminescence (PerkinElmer, Crofton, MD). Relative protein levels were determined by densitometric analysis of immunoreactive bands and normalized to total α-tubulin levels.

Cell fractionation

WIF-B cells grown on 10-cm dishes were detached with trypsin for 2 min at 37 °C and pelleted by centrifugation. Cells were resuspended in 5–8 ml ice-cold swelling buffer (1 mM $MgCl_2$, 1 mM DTT, 1 mM EDTA) and incubated 5 min on ice. Cells were pelleted by centrifugation and resuspended in 500 μl of 0.25 M sucrose, 3 mM imidazole, pH 7.4 with added protease inhibitors (2 μg/ml each of leupeptin, antipain, PMSF and benzamidine) and Dounce-homogenized with a tight fitting pestle for 20 strokes. The homogenate was centrifuged at $1,000 \times g$ at 4 °C for 5 min to prepare a post-nuclear supernatant (PNS). The PNS was centrifuged at $20,000 \times g$ for 20 min at 4 °C to prepare a heavy membrane population. The resultant supernatant was then centrifuged at $80,000 \times g$ for 60 min at 4 °C to prepare cytosolic and light membrane fractions. The fractions were immunoblotted for dynein, p150, and α-tubulin, and their relative distributions were determined by densitometry.

Microtubule binding

Microtubules were purified as we have described [17]. Briefly, detached cells grown on 10-cm dishes that were swollen and recovered as described above were Dounce-homogenized in 0.5–1.0 ml PEM (100 mM Pipes, 1 mM EGTA, 1 mM $MgSO_4$, pH 6.6) with added protease inhibitors (2 μg/ml each of leupeptin, antipain, PMSF and benzamidine). The homogenate was centrifuged at $1,000 \times g$ at 4 °C for 5 min to prepare a PNS. The PNS was centrifuged for 20 min at 4 °C at $20,000 \times g$. 100 μM taxol was added to the supernatant for 15 min at 37 °C to polymerize microtubules. The microtubules were pelleted through a 10 % sucrose cushion at $150,000 \times g$ at 20 °C for 30 min. The resultant supernatant and pelleted fraction (containing microtubules and associated proteins) were immunoblotted for dynein, p150, and α-tubulin. The distributions of the proteins in the soluble or pelleted fractions were determined by densitometry.

Statistical analysis

Results were expressed as the mean ± S.E.M from at least three independent experiments. Comparisons between control and ethanol-treated cells were made using the Student's t test for paired data. p values 0.05 were considered significant.

Results

Ethanol impairs basolateral to canalicular transcytosis

To determine whether transcytosis is impaired in ethanol-treated cells, we monitored the trafficking of basolaterally labeled canalicular proteins. Importantly, we selected a representative of each of three classes of transcytosing hepatic canalicular proteins: (1) aminopeptidase *N* (APN), a single spanning membrane protein; (2) 5′nucleotidase (5′NT), a lipid-anchored protein; and (3) polymeric IgA receptor (pIgA-R), a so-called "professional transcytosing" protein, i.e., a protein that transcytoses in all epithelial cell types. After preincubation with ethanol for 72 h, the canalicular proteins were basolaterally labeled with antibodies specific to their external epitopes for 20 min at 4 °C in the continued absence or presence of ethanol. The antibody-antigen complexes were chased to the canalicular surface for 45 min at 37 °C, and the cells were fixed and processed for immunofluorescence detection of the trafficked proteins. Because tight junctions restrict antibody access to the canalicular surface, only basolateral labeling was detected after 0 min of chase in control and ethanol-treated cells (Fig. 1A). After 45 min of chase, robust apical labeling was observed in control cells indicating successful canalicular delivery (Fig. 1B). In contrast, significantly decreased canalicular labeling was observed in ethanol-treated cells with a reciprocal increase in intracellular labeling on sub-canalicular structures (Fig. 1B).

To confirm the morphological observations, we quantitated the canalicular versus basolateral distributions from micrographs using our previously published method [14]. As shown in Fig. 2, there was a significant decrease in canalicular delivery for all three markers in ethanol-treated cells. Notably, the impairment observed for pIgA-R and APN was about twice that observed for 5′NT. Both pIgA-R and APN are basolaterally internalized via clathrin-mediated endocytosis, a process we have shown is selectively impaired by ethanol exposure [18, 19]. In contrast, 5′NT is internalized via a "raft"-mediated process that is not altered in ethanol-treated cells. Thus, the smaller, yet significant impairment observed for 5′NT can be explained by altered vesicle trafficking along hyperacetylated microtubule tracks, while the larger impairments for APN and pIgA-R likely reflect the additive defects in vesicle trafficking and internalization.

To confirm that our observations are not specific to the WIF-B cells, we examined canalicular protein trafficking in the hepatic VL-17A cells. Importantly, these cells have been engineered to stably express both ADH and CYP2E1 and efficiently metabolize ethanol in culture [12]. However, these cells do not polarize in culture so they do not exhibit transcytosis *per se*. Rather canalicular proteins are delivered from the cell surface to a so-called canalicular/apical compartment. We have characterized this pathway extensively in other nonpolarized, hepatic-derived cell lines [20]. As in polarized cells, the canalicular proteins are selectively internalized from the cell surface and delivered to structures containing only other canalicular/apical proteins (the canalicular/apical compartment). In the absence of canalicular retention mechanisms at this compartment, the canalicular proteins recycle to the cell surface. To avoid confounding results from recycling, pIgA-R trafficking from the plasma membrane to the canalicular/apical compartment was monitored for only 15 min, a time interval that allows compartment delivery, but precedes surface recycling. As

shown in Fig. 3, in both control and ethanol-treated VL-17A cells, pIgA-R was only detected at the surface after antibody labeling for 20 min at 4 °C. After 15 min of chase, pIgA-R was detected in the juxta-nuclear, canalicular/apical compartment (two examples are shown in Fig. 3b, c). In contrast and consistent with results from Figs. 1 and 2, no intracellular labeling was detected in ethanol-treated cells indicating impaired delivery (Fig. 3e). To quantitate the relative levels of canalicular protein trafficking, we counted the pIgA-R-expressing cells that contained intracellular labeling versus the total number of cells. We determined that after 0 min of chase, 0 % of pIgA-R-expressing cells were positive for intracellular staining for both control and ethanol-treated cells. However, after 15 min, 23 % of control cells were positive, whereas only 6 % were positive in ethanol-treated cells indicating impaired delivery. Thus, alcohol-induced defects in apical protein trafficking are not specific to WIF-B cells.

Transcytosing proteins are present on sub-canalicular structures that align with acetylated microtubules and colocalize with dynein/dynactin

Because WIF-B cells can both metabolize ethanol and polarize in culture, we continued our studies on ethanol-induced impairments in transcytosis in WIF-B cells. When viewing micrographs of transcytosing proteins en route to the canalicular surface at higher magnification, fluorescence is only detected at the canalicular surface in control cells (Fig. 4A). However in ethanol-treated cells, we noticed that each transcytosing protein was additionally detected in clusters of puncta (marked with arrows) or single, discrete puncta (marked with arrowheads) en route to the canalicular surface suggesting their presence in stalled vesicles (Fig. 4A) (compare panels a–c to d–f). To determine whether these vesicles were stalled along acetylated microtubules in ethanol-treated cells, we labeled cells for acetylated α-tubulin at steady state and for transcytosing APN. As we have previously shown [3], the acetylated tubulin polymers were clustered around the canalicular surface and extended into the cell periphery as short, gnarled tubules (Fig. 4B). In ethanol-treated cells, increased acetylated microtubules were observed as we have also previously shown, and the APN-positive puncta aligned along or were immediately adjacent to the acetylated microtubules (Fig. 4B) suggesting that transcytosing vesicles are stalled on the acetylated polymers. No such overlap was detected in control cells (Fig. 4B).

If the puncta represent stalled vesicles in ethanol-treated cells, one prediction is that the distributions of the minus-end directed microtubule motor, dynein, and its activating complex, dynactin, are also more punctate in ethanol-treated cells. To test this possibility, we immunolabeled control and ethanol-treated cells for the intermediate chain of dynein and the p150^{glued} (p150) subunit of dynactin. As shown in Fig. 5A, the predicted redistribution was observed. In control cells, both dynein and p150 staining was diffuse and uniformly distributed throughout the cytoplasm. Although a substantial diffuse cytosolic pool was remained in ethanol-treated cells, dynein and p150-positive puncta were also readily apparent. Interestingly, these ethanol-induced puncta were more concentrated at or near the canalicular surface, the subcellular site where acetylated microtubules are also concentrated [3].

At higher magnification (Fig. 5A), the puncta are more apparent and discrete and resemble the stalled transcytotic vesicles (marked with arrows). To determine whether dynein/ dynactin is present on the canaliculi-destined vesicles, ethanol-treated cells were double-labeled for steady state dynein or p150 distributions with transcytosing APN. As shown in Fig. 5B, sub-canalicular puncta or at the canalicular surface (marked with arrows) indicating that both dynein and dynactin are present on the stalled vesicles.

Dynein binds microtubules more tightly in ethanol-treated cells

To determine whether decreased canalicular delivery in ethanol-treated cells is simply the result of decreased dynein/dynactin expression levels, we immunoblotted whole cell extracts from control and treated cells. No significant changes in dynactin expression levels were observed (101 ± 4.0 % of control) (Fig. 6A). Although dynein expression levels were reduced to 81 ± 2.0 % of control (Fig. 6A), this decrease was not significant and likely cannot account for the greater than 50 % impairment in transcytosis observed for APN and pIgA-R.

To determine whether decreased dynein/dynactin vesicle binding is responsible for impaired canalicular delivery, we prepared cytosolic (S3), heavy (P2), and light membrane (P3) fractions from control or ethanol-treated cells and immuno-blotted for dynein or p150. A representative immunoblot for each antigen is shown in Fig. 6B. From densitometric analysis of several experiments, we determined that in control cells, the majority of dynein was detected in the cytosolic fraction (76.1 ± 6.2 % of total) with a small sub-population detected in the light membrane fraction (23.9 ± 16.2 %) (Table 1). In contrast, much more p150 was membrane associated with 19.5 ± 7.1 % of total in the heavy membrane fractions and 38.8 ± 1.5 % in the light membrane fraction. These results are consistent with a current model for dynein/dynactin structure where dynein mediates transient associations with microtubules and dynactin mediates vesicle attachment [21]. In ethanol-treated cells, these distributions were not altered; dynein remained mainly cytosolic (81.0 ± 19.0 % of total) and p150 remained on the vesicle fractions (18.7 ± 9.5 and 30.5 ± 10.2 % in the heavy and light membrane fractions, respectively) (Table 1). For comparison, we determined that α-tubulin was mainly soluble in both preparations with 93.5 ± 6.5 and 98.2 ± 1.8 % in the cytosolic fraction from control and ethanol-treated cells, respectively. Thus, ethanol exposure did not alter membrane binding of dynein/dynactin.

To determine whether dynein/dynactin microtubule associations were altered, we performed microtubule binding assays. Taxol-stabilized polymers were purified by centrifugation through a sucrose cushion as we have described [17], and samples were immunoblotted for dynein, p150, and α-tubulin. A representative immunoblot for each antigen is shown in Fig. 6C. As we have shown [17], polymerized microtubules are efficiently recovered from both control and ethanol-treated cells. Densitometric analysis of the fractions after correcting for volume revealed that in control cells, only 25.5 ± 6.1 % of total p150 co-pelleted with microtubules, and in ethanol-treated cells, the amount recovered did not significantly change (17.5 ± 2.6 %) (Table 2). In contrast, alcohol exposure significantly enhanced dynein associations with microtubules from 16.7 ± 1.5 % in control to 100 ± 0.0 % (p 0.001) of total dynein in ethanol-treated samples (Fig. 6C; Table 2). Thus, we conclude that ethanol-

induced hyperacetylation leads to enhanced dynein binding to microtubules that leads to stalled transcytotic vesicles and impaired transcytosis.

Discussion

Here we report that basolateral to canalicular transcytosis is impaired by ethanol exposure in polarized, hepatic WIF-B cells. Unlike in control cells, transcytosing vesicles accumulated sub-canalicularly and aligned along or just adjacent to acetylated microtubules. Both the minus-end directed motor, dynein, and its activating complex, dynactin, colocalized with the transcytosing proteins suggesting the vesicles were stalled. Consistent with reports from other cell types, dynein (but not dynactin) more tightly associates with microtubules from ethanol-treated cells than from control. From these results, we propose that enhanced motor binding to microtubules in ethanol-treated cells leads to decreased motor processivity resulting in vesicle stalling and ultimately, in impaired delivery.

The WIF-B cells: a powerful model system for the study of alcohol-induced hepatotoxicity

Although animal models have been used to describe hepatic responses to alcohol consumption, there are disadvantages to using these models. Not only is there considerable physiologic variation among animals, it is also difficult to quickly alter experimental parameters (e.g., inhibitor addition, temperature changes) that are required for mechanistic studies. Furthermore, experimental compounds are introduced to all body organs that may interfere with defining hepatic-specific responses or produce severe side effects. Established in vitro systems present other challenges. For example, within hours of culture, isolated hepatocytes lose their liver-specific functions and surface polarity. Similarly, hepatic/ hepatoma-derived cells (e.g., Clone 9, HepG2 and HuH7 cells) are nonpolarized and de-differentiated in culture.

In contrast, cultured WIF-B cells enter a terminal differentiation program. After 7-10 days in culture, 70–95 % of WIF-B cells are fully differentiated and exhibit phase-lucent structures that are functionally and compositionally analogous to bile canaliculi [10]. Domain-specific membrane proteins are localized in WIF-B cells as they are in hepatocytes in situ, and liver-specific functions are maintained [13, 22]. Importantly for our studies, WIF-B cells efficiently metabolize ethanol using endogenous ADH and CYP2E1 [2]. Like hepatocytes in situ, ethanol-treated WIF-B cells have an increased redox state, increased triglycerides, enhanced lipid droplet formation, and produce reactive oxygen species [1, 2]. Our studies have further demonstrated that WIF-B cells display alcohol-induced defects in cellular processes as described in situ or in isolated hepatocytes. These impairments include impaired microtubule polymerization, and defects in asialoglyco-protein receptor trafficking, clathrin-mediated internalization, and albumin secretion [3, 9, 18, 19]. We believe these properties argue strongly that WIF-B cells are an excellent model for the examination of alcohol-induced hepatotoxicity and allow for meaningful mechanistic studies.

Transcytotic vesicles are stalled along acetylated microtubules in ethanol-treated cells

The enhanced punctate colocalization of the trafficking canalicular proteins and dynein/ dynactin complexes with acetylated tubulin suggests that the transcytotic vesicles are stalled in ethanol-treated cells at sites of hyper-modified microtubules. This is consistent with live cell imaging studies in isolated hepatocytes from ethanol-treated rats where a significant decrease in vesicle motility was observed [23]. Because no differences in dynein protein expression levels, membrane association, or ATPase activity were observed in the ethanol-exposed isolated hepatocytes [23], the authors were unable to account for the impaired motility. Our findings suggest that ethanol-induced microtubule acetylation is a likely explanation.

Although there is an expanding list of proteins that are known to be hyperacetylated upon ethanol exposure [24], little is known about the functional consequences of this modification. The added acetyl group likely neutralizes the positive charge on lysine while increasing the overall size and hydrophobicity of the side chain. Such changes may result in protein conformational changes that alter function. Although the acetylated residue in α-tubulin (lysine 40) resides in the microtubule lumen [25], our studies and studies from others have shown that both dynein and kinesin (a plus-end directed microtubule motor) preferentially bind acetylated microtubules [26–28]. However, enhanced microtubule acetylation has been correlated with enhanced kinesin-based neuronal anterograde transport [27]. More recently, in vitro studies with purified proteins demonstrated that tubulin acetylation *alone* cannot enhance kinesin velocity or run length [29] indicating that the situation in vivo is more complicated.

We suggest that the microtubule environment is even more "complicated" in ethanol-treated hepatocytes. We have shown that lysine 40 acetylation on α-tubulin is enhanced in ethanol exposed WIF-B cells, VL-17A cells, liver slices, and in livers from ethanol-fed rats [3, 5]. Recent studies have confirmed an acetylated site in β-tubulin (lysine 252) and a proteomics screen identified 8 other candidate lysines on α-tubulin and 1 on β-tubulin [30, 31]. It is not yet known whether ethanol enhances acetylation of any of these residues. Furthermore, tubulin, purified hepatic microtubule associated proteins, and motors have all been shown to form adducts with acetaldehyde in vitro [32, 33] suggesting these modifications may also contribute to impaired microtubule and/or vesicle dynamics. Clearly, studies are needed to determine what modification or combination of modifications leads to impaired protein trafficking.

Novel therapeutic targets for treating alcohol-induced liver injury

Although progression of alcoholic liver disease is clinically well described proceeding from steatosis to fibrosis and finally to cirrhosis, there are no treatments available for the alcoholic patient to alleviate or reverse the disease state. Thus, we argue it is important to actively investigate other possible mechanisms that contribute to the observed clinical pathologies or may contribute to other, less understood mechanisms of hepatotoxicity that may then be targeted for the development of novel therapeutic strategies. Our studies importantly suggest that modulating cellular acetylation levels is one such unique therapeutic target. To date, the acetylation of numerous proteins is known to be enhanced by

ethanol treatment [24]. Currently, specific naturally occurring and synthetic deacetylase agonists are well tolerated in humans and are in clinical trials for treatment of inflammation, metabolic disorders (e.g., type II diabetes), cardio-vascular, and neurodegenerative diseases [34]. One such agent, resveratrol, has also been shown to attenuate fatty liver and oxidative stress in alcohol-exposed mice [35]. However, these agonists are all targeted to SirT1, a class III nuclear deacetylase and likely act by altering gene expression. Because alcohol induces the hyperacetylation of a host of mitochondrial and cytosolic proteins [24, 36, 37], the identification of agonists to the major cytoplasmic (HDAC6) or mitochondrial (SirT3, 4 and 5) deacetylases may alleviate oxidative stress or protein trafficking defects without altering gene expression thereby potentially reducing side effects.

Acknowledgements

Abbreviations

5′NT	5′Nucleotidase
ADH	Alcohol dehydrogenase
APN	Aminopeptidase N
CYP2E1	Cytochrome P_{450} 2E1
pIgA-R	Polymeric IgA receptor

References

1. McVicker BL, Tuma PL, Kharbanda KK, Lee SM, Tuma DJ. Relationship between oxidative stress and hepatic glutathione levels in ethanol-mediated apoptosis of polarized hepatic cells. World J Gastroenterol. 2009; 15:2609–2616. [PubMed: 19496190]

2. Schaffert CS, Todero SL, McVicker BL, Tuma PL, Sorrell MF, Tuma DJ. WIF-B cells as a model for alcohol-induced hepatocyte injury. Biochem Pharmacol. 2004; 67:2167–2174. [PubMed: 15135311]

3. Kannarkat GT, Tuma DJ, Tuma PL. Microtubules are more stable and more highly acetylated in ethanol-treated hepatic cells. J Hepatol. 2006; 44:963–970. [PubMed: 16169115]

4. Westermann S, Weber K. Post-translational modifications regulate microtubule function. Nat Rev Mol Cell Biol. 2003; 4:938–947. [PubMed: 14685172]

5. Fernandez DJ, Tuma DJ, Tuma PL. Hepatic microtubule acetylation and stability induced by chronic alcohol exposure impair nuclear translocation of stat3 and stat5b, but not smad2/3. Am J Physiol Gastrointest Liver Physiol. 2012; 303(12):G1402–G1415. [PubMed: 23064763]

6. Mizuno M, Singer SJ. A possible role for stable microtubules in intracellular transport from the endoplasmic reticulum to the Golgi apparatus. J Cell Sci. 1994; 107(Pt 5):1321–1331. [PubMed: 7929638]

7. Pous C, Chabin K, Drechou A, Barbot L, Phung-Koskas T, Settegrana C, et al. Functional specialization of stable and dynamic microtubules in protein traffic in WIF-B cells. J Cell Biol. 1998; 142:153–165. [PubMed: 9660870]

8. Phung-Koskas T, Pilon A, Pous C, Betzina C, Sturm M, Bourguet-Kondracki ML, et al. STAT5B-mediated growth hormone signaling is organized by highly dynamic microtubules in hepatic cells. J Biol Chem. 2005; 280:1123–1131. [PubMed: 15528207]

9. Joseph RA, Shepard BD, Kannarkat GT, Rutledge TM, Tuma DJ, Tuma PL. Microtubule acetylation and stability may explain alcohol-induced alterations in hepatic protein trafficking. Hepatology. 2008; 47:1745–1753. [PubMed: 18161881]

10. Shanks MR, Cassio D, Lecoq O, Hubbard AL. An improved polarized rat hepatoma hybrid cell line. Generation and comparison with its hepatoma relatives and hepatocytes in vivo. J Cell Sci. 1994; 107(Pt 4):813–825. [PubMed: 8056838]

11. Bastaki M, Braiterman LT, Johns DC, Chen YH, Hubbard AL. Absence of direct delivery for single transmembrane apical proteins or their "Secretory" forms in polarized hepatic cells. Mol Biol Cell. 2002; 13:225–237. [PubMed: 11809835]

12. Donohue TM, Osna NA, Clemens DL. Recombinant Hep G2 cells that express alcohol dehydrogenase and cytochrome P450 2E1 as a model of ethanol-elicited cytotoxicity. Int J Biochem Cell Biol. 2006; 38:92–101. [PubMed: 16181800]

13. Ihrke G, Neufeld EB, Meads T, Shanks MR, Cassio D, Laurent M, et al. WIF-B cells: an in vitro model for studies of hepatocyte polarity. J Cell Biol. 1993; 123:1761–1775. [PubMed: 7506266]

14. Nyasae LK, Hubbard AL, Tuma PL. Transcytotic efflux from early endosomes is dependent on cholesterol and glycosphingolipids in polarized hepatic cells. Mol Biol Cell. 2003; 14:2689–2705. [PubMed: 12857857]

15. Ramnarayanan SP, Cheng CA, Bastaki M, Tuma PL. Exogenous MAL reroutes selected hepatic apical proteins into the direct pathway in WIF-B cells. Mol Biol Cell. 2007; 18:2707–2715. [PubMed: 17494867]

16. Laemmli UK. Cleavage of structural proteins during the assembly of the head of bacteriophage T4. Nature. 1970; 227:680–685. [PubMed: 5432063]

17. Shepard BD, Joseph RA, Kannarkat GT, Rutledge TM, Tuma DJ, Tuma PL. Alcohol-induced alterations in hepatic micro-tubule dynamics can be explained by impaired histone deacetylase 6 function. Hepatology. 2008; 48(5):1671–1679. [PubMed: 18697214]

18. Fernandez DJ, McVicker BL, Tuma DJ, Tuma PL. Ethanol selectively impairs clathrin-mediated internalization in polarized hepatic cells. Biochem Pharmacol. 2009; 78:648–655. [PubMed: 19463792]

19. Shepard BD, Tuma DJ, Tuma PL. Lysine acetylation induced by chronic ethanol consumption impairs dynamin-mediated clathrin-coated vesicle release. Hepatology. 2012; 55:1260–1270. [PubMed: 22095875]

20. Tuma PL, Nyasae LK, Hubbard AL. Nonpolarized cells selectively sort apical proteins from cell surface to a novel compartment, but lack apical retention mechanisms. Mol Biol Cell. 2002; 13:3400–3415. [PubMed: 12388745]

21. Kardon JR, Vale RD. Regulators of the cytoplasmic dynein motor. Nat Rev Mol Cell Biol. 2009; 10:854–865. [PubMed: 19935668]

22. Griffo G, Hamon-Benais C, Angrand PO, Fox M, West L, Lecoq O, et al. HNF4 and HNF1 as well as a panel of hepatic functions are extinguished and reexpressed in parallel in chromosomally reduced rat hepatoma-human fibroblast hybrids. J Cell Biol. 1993; 121:887–898. [PubMed: 8491780]

23. Torok N, Marks D, Hsiao K, Oswald BJ, McNiven MA. Vesicle movement in rat hepatocytes is reduced by ethanol exposure: alterations in microtubule-based motor enzymes. Gastroenterology. 1997; 113:1938–1948. [PubMed: 9394734]

24. Shepard BD, Tuma PL. Alcohol-induced protein hyper-acetylation: mechanisms and consequences. World J Gastroenterol. 2009; 15:1219–1230. [PubMed: 19291822]

25. Nogales E, Whittaker M, Milligan RA, Downing KH. High-resolution model of the microtubule. Cell. 1999; 96:79–88. [PubMed: 9989499]

26. Liao G, Gundersen GG. Kinesin is a candidate for cross-bridging microtubules and intermediate filaments. Selective binding of kinesin to detyrosinated tubulin and vimentin. J Biol Chem. 1998; 273:9797–9803. [PubMed: 9545318]

27. Reed NA, Cai D, Blasius TL, Jih GT, Meyhofer E, Gaertig J, et al. Microtubule acetylation promotes kinesin-1 binding and transport. Curr Biol. 2006; 16:2166–2172. [PubMed: 17084703]

28. Dompierre JP, Godin JD, Charrin BC, Cordelieres FP, King SJ, Humbert S, et al. Histone deacetylase 6 inhibition compensates for the transport deficit in Huntington's disease by increasing tubulin acetylation. J Neurosci. 2007; 27:3571–3583. [PubMed: 17392473]

29. Walter WJ, Beranek V, Fischermeier E, Diez S. Tubulin acetylation alone does not affect kinesin-1 velocity and run length in vitro. PLoS One. 2012; 7:e42218. [PubMed: 22870307]

30. Choudhary C, Kumar C, Gnad F, Nielsen ML, Rehman M, Walther TC, et al. Lysine acetylation targets protein complexes and co-regulates major cellular functions. Science. 2009; 325:834–840. [PubMed: 19608861]

31. Chu CW, Hou F, Zhang J, Phu L, Loktev AV, Kirkpatrick DS, et al. A novel acetylation of beta-tubulin by San modulates microtubule polymerization via down-regulating tubulin incorporation. Mol Biol Cell. 2011; 22:448–456. [PubMed: 21177827]

32. Jennett RB, Sorrell MF, Johnson EL, Tuma DJ. Covalent binding of acetaldehyde to tubulin: evidence for preferential binding to the alpha-chain. Arch Biochem Biophys. 1987; 256:10–18. [PubMed: 3606116]

33. Jennett RB, Sorrell MF, Saffari-Fard A, Ockner JL, Tuma DJ. Preferential covalent binding of acetaldehyde to the alpha-chain of purified rat liver tubulin. Hepatology. 1989; 9:57–62. [PubMed: 2908869]

34. Elliott PJ, Jirousek M. Sirtuins: novel targets for metabolic disease. Curr Opin Investig Drugs. 2008; 9:371–378.

35. Ajmo JM, Liang X, Rogers CQ, Pennock B, You M. Resveratrol Alleviates Alcoholic Fatty Liver in Mice. Am J Physiol Gastrointest Liver Physiol. 2008; 295(4):G833–G842. [PubMed: 18755807]

36. Shepard BD, Tuma DJ, Tuma PL. Chronic Ethanol Consumption Induces Global Hepatic Protein Hyperacetylation. Alcohol Clin Exp Res. 2010; 34:280–291. [PubMed: 19951295]

37. Picklo MJ Sr. Ethanol intoxication increases hepatic N-lysyl protein acetylation. Biochem Biophys Res Commun. 2008; 376(3):615–619. [PubMed: 18804449]
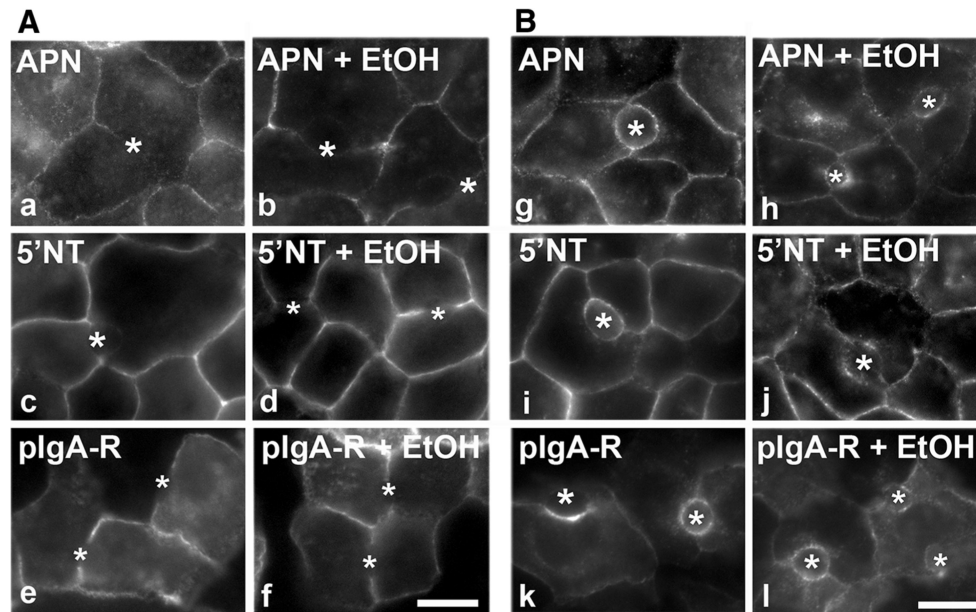
Fig. 1.
Basolateral to canalicular transcytosis is impaired in ethanol-treated cells. WIF-B cells were treated in the absence or presence of 50 mM ethanol (EtOH) for 72 h as indicated. Live cells were basolaterally labeled for the indicated canalicular proteins with specific antibodies for 20 min at 4 °C. After washing away excess antibodies, antibody-antigen complexes were chased for 0 (A, *a–f*) or 45 min (B, *g–l*) at 37 °C in the continued absence or presence ethanol. Cells were fixed and permeabilized and labeled with secondary antibodies to detect the transcytosed proteins. *Bar* 10 μm. *Asterisks* are marking selected bile canaliculi
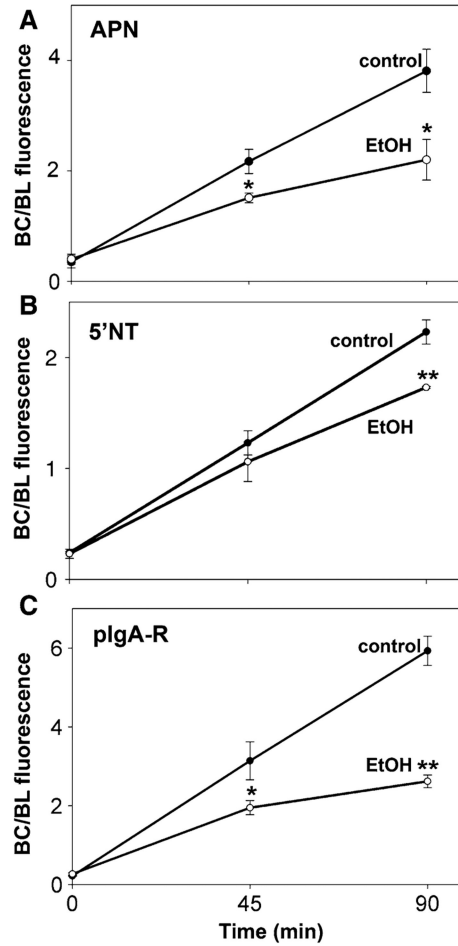
Fig. 2.
Transcytosis of pIgA-R is impaired to the greatest extent in ethanol-treated cells. WIF-B cells were treated in the absence or presence of 50 mM ethanol (EtOH) for 72 h as indicated. Live cells were basolaterally labeled for the indicated canalicular proteins as described in Fig. 1 and chased for 0, 45, or 90 min at 37 °C in the continued absence or presence ethanol. Cells were fixed and permeabilized and labeled with secondary antibodies to detect the transcytosed proteins. Random fields were visualized by epifluorescence and digitized. From micrographs, the average pixel intensity of each marker at selected regions of interest placed at the bile canalicular or basolateral membrane of the same WIF-B cell was measured. The averaged *background pixel* intensity was subtracted from each value, and the ratio of bile canalicular (BC) to basolateral (BL) fluorescence intensity was determined. Values are expressed as the mean ± SEM for APN (**A**), 5′NT (**B**), and pIgA-R (**C**). Measurements were performed on at least three independent experiments. *p 0.05, **p 0.005
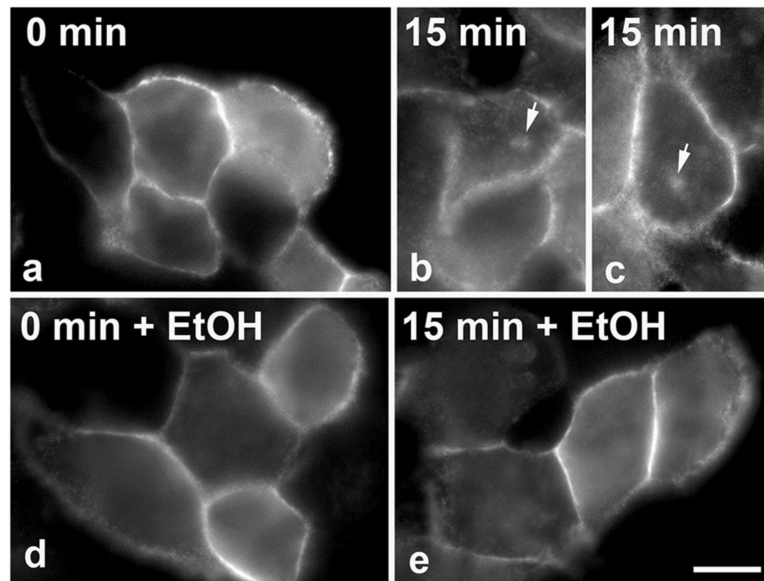
Fig. 3.
Canalicular protein trafficking is impaired in VL-17A cells. VL-17A cells expressing pIgA-R were treated in the absence or presence of 50 mM ethanol (EtOH) for 24 h as indicated. Live cells were basolaterally labeled for pIgA-R with specific antibodies for 20 min at 4 °C. After washing away excess antibodies, antibody-antigen complexes were chased for 0 (**a, d**) or 15 min (**b, c, e**) at 37 °C in the continued absence or presence ethanol. Cells were fixed and permeabilized and labeled with secondary antibodies to detect the transcytosed proteins. *Bar* 10 μm. *Arrows* are marking the canalicular/apical compartment in control cells
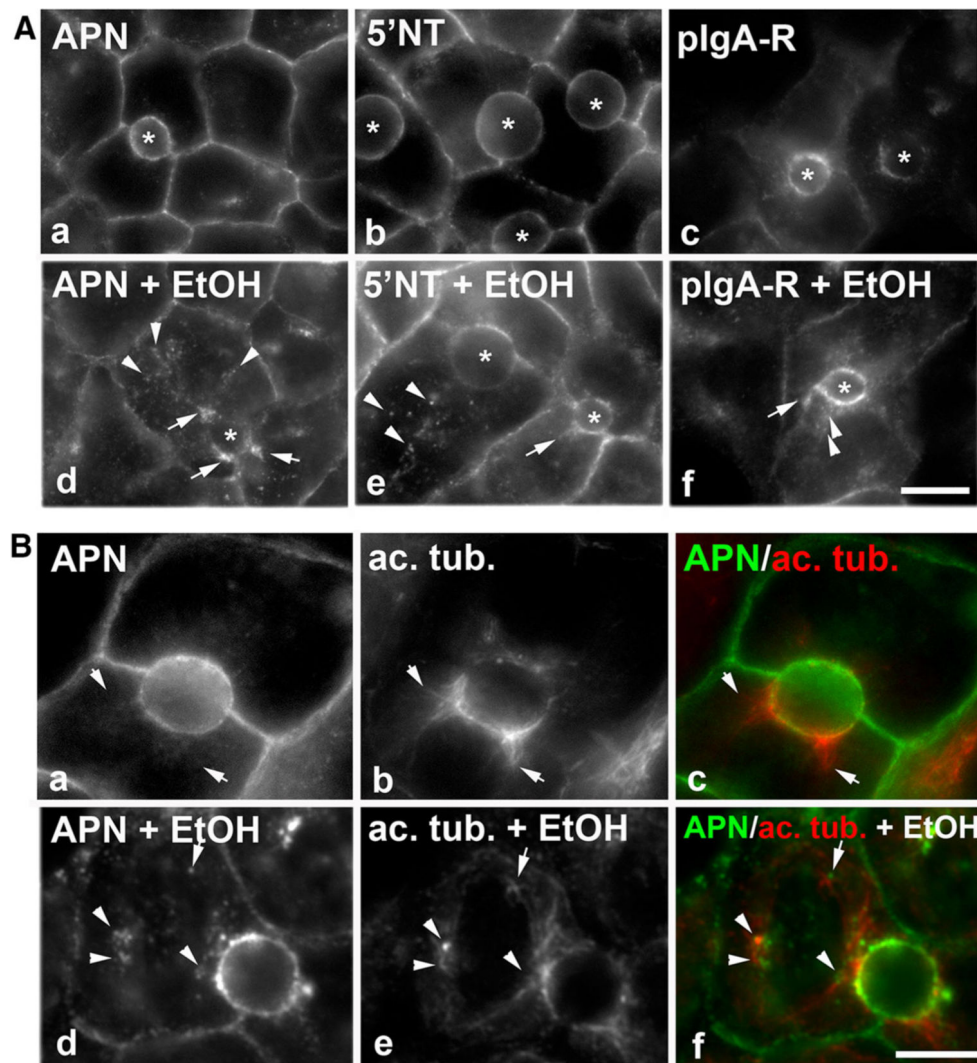
Fig. 4.
Transcytosing proteins are present on sub-canalicular structures that are aligned along acetylated microtubules in ethanol-treated cells. **A, B** Cells were treated in the absence (*a–c*) or presence of 50 mM ethanol (EtOH) (*d–f*) for 72 h as indicated. Live cells were labeled with the indicated canalicular proteins as described in Fig. 1, and the antibody-antigen complexes chased for 45 min. The transcytosing proteins are additionally detected in sub-canalicular clusters (marked with *arrows*) or discrete puncta (marked with *arrow heads*) in ethanol-treated cells (*d–f*). Bar 10 μm. In **B**, APN antibody-antigen complexes were continuously chased for 45 min and cells processed for immunofluorescence detection of both the trafficked APN and acetylated α-tubulin. Merged images are shown in *c* and *f*. *Arrows* are pointing to APN-positive structures that are immediately adjacent to acetylated microtubules in ethanol-treated cells. *Bar* 10 μm
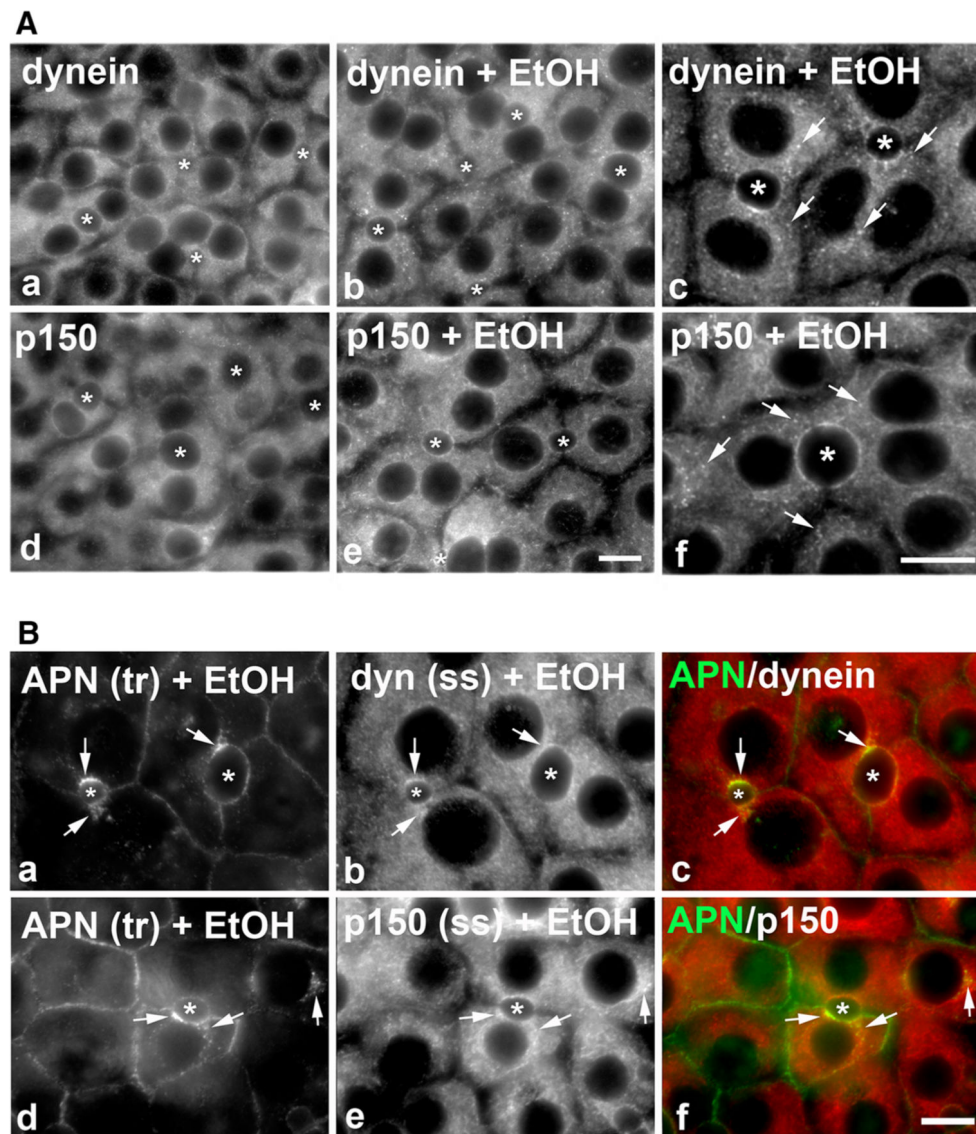
Fig. 5.
Dynein and dynactin colocalize with stalled transcytosing proteins. **A** WIF-B cells were treated in the absence or presence of 50 mM ethanol (EtOH) for 72 h and labeled for dynein intermediate chain (dyn) and p150 as indicated. In the higher magnification images (*c* and *f*), arrows mark discrete puncta observed only in ethanol-treated cells. *Asterisks* mark selected bile canaliculi. *Bar* 10 μm. **B** WIF-B cells were treated with 50 mM ethanol (EtOH) for 72 h. APN was continuously basolaterally labeled for 45 min and cells processed for immunodetection of trafficked (tr) APN and steady state (ss) dynein (dyn) (*a–c*) or p150 (*d–f*). Merged images are shown in *c* and *f*. *Arrows* point to regions of colocalization. *Bar* 10 μm
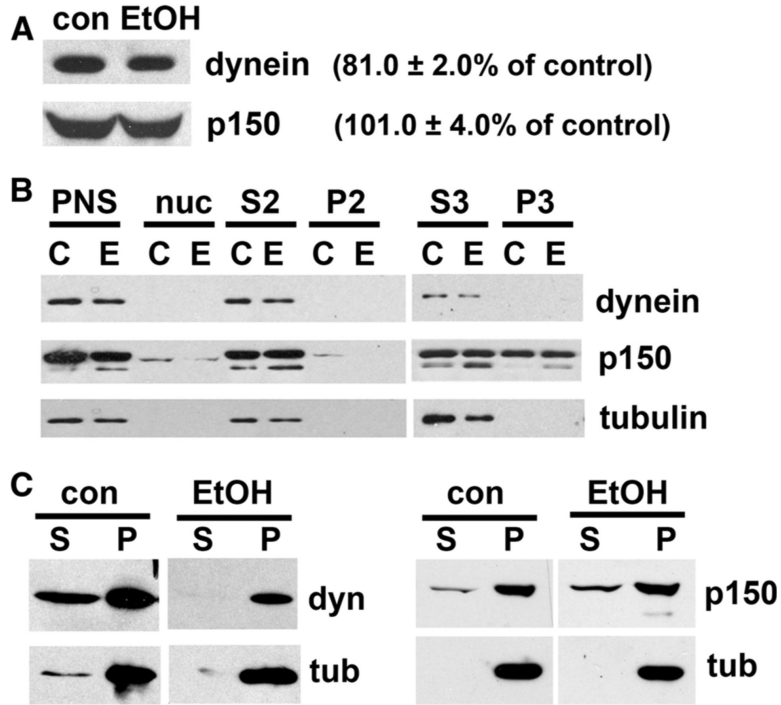
Fig. 6.
Ethanol does not significantly alter dynein or dynactin protein expression levels or membrane attachment but enhances dynein microtubule binding. **A** Whole cell lysates from control (con) or treated (EtOH) cells were immunoblotted for dynein intermediate chain (dyn) or p150. Relative levels were determined with densitometry and normalized to total α-tubulin. Values indicate the percent expression in ethanol-treated cells relative to control and are the mean ± SEM from at least four independent experiments. **B** Post-nuclear supernatants (PNS), nuclear pellets (nuc) and cytosolic (S3), heavy (P2), and light membrane (P3) fractions from control or ethanol-treated cells (see "Materials and methods" section) were immunoblotted for dynein intermediate chain (dyn), p150, or atubulin (tub). Representative immunoblots are shown. **C** Polymerized microtubules were pelleted from cytosolic extracts (see "Materials and methods" section) from control or ethanol (EtOH) treated cells. The supernatant (S) and microtubule pellet (P) were immunoblotted for dynein intermediate chain (dyn), p150, or α-tubulin (tub). Representative immunoblots are shown

Table 1

Ethanol treatment does not alter dynein/dynactin membrane attachment

| | % Distribution | | | | | |
| | **Dynein** | | **p150** | | **α-Tubulin** | |
	Con	**EtOH**	**Con**	**EtOH**	**Con**	**EtOH**
P_2	0.0 ± 0.0	0.0 ± 0.0	19.5 ± 7.1	18.7 ± 9.5	4.8 ± 4.8	1.8 ± 1.8
S_3	76.1 ± 6.2	81.0 ± 19.0	41.8 ± 5.9	50.8 ± 6.9	93.5 ± 6.5	98.2 ± 1.8
P_3	23.9 ± 16.2	19.0 ± 19.0	38.8 ± 1.5	30.5 ± 10.2	1.7 ± 1.7	0.0 ± 0.0

Membrane fractions (see "Materials and methods" section) were immunoblotted for dynein intermediate chain, p150 or α-tubulin as indicated. Relative protein distributions in the cytosol (S3) and the heavy (P2) and light (P3) membrane fractions were determined by densitometric analysis of immunoreactive bands. Values are expressed as the mean ± SEM and were determined from at least three independent experiments

Table 2

Dynein binds microtubules more tightly in ethanol-treated cells

	Percent Microtubule Associated	
	Con	EtOH
Dynein	16.7 ± 1.5	100.0 ± 0.0[*]
p150	25.5 ± 6.1	17.5 ± 2.6

Microtubules were polymerized and pelleted from cytosolic extracts (see "Materials and methods" section) from control or ethanol (EtOH) treated cells. The supernatant and microtubule pellet were immunoblotted for dynein intermediate chain and p150. The percent of pelleted protein was determined by densitometric analysis of immunoreactive bands and values corrected for volume. Values are expressed as the mean ± SEM and were determined from at least three independent experiments.

[*] p 0.001